Imaging of Titan from the Cassini spacecraft

Carolyn C. Porco[1], Emily Baker[1], John Barbara[2], Kevin Beurle[3], Andre Brahic[4], Joseph A. Burns[5], Sebastien Charnoz[4], Nick Cooper[3], Douglas D. Dawson[6], Anthony D. Del Genio[2], Tilmann Denk[7], Luke Dones[8], Ulyana Dyudina[9], Michael W. Evans[3], Stephanie Fussner[6], Bernd Giese[10], Kevin Grazier[11], Paul Helfenstein[5], Andrew P. Ingersoll[9], Robert A. Jacobson[11], Torrence V. Johnson[11], Alfred McEwen[6], Carl D. Murray[3], Gerhard Neukum[7], William M. Owen[11], Jason Perry[6], Thomas Roatsch[10], Joseph Spitale[1], Steven Squyres[5], Peter Thomas[5], Matthew Tiscareno[5], Elizabeth P. Turtle[6], Ashwin R. Vasavada[11], Joseph Veverka[5], Roland Wagner[10] & Robert West[11]

[1]*Cassini Imaging Central Laboratory for Operations, Space Science Institute, 4750 Walnut Street, Suite 205, Boulder, Colorado 80301, USA*
[2]*NASA Goddard Institute for Space Studies, 2880 Broadway, New York, New York 10025, USA*
[3]*Astronomy Unit, Queen Mary, University of London, London E1 4NS, UK*
[4]*C.E. de Saclay, Université Paris 7, L'Orme des Merisiers, 91191 Gif-sur-Yvette Cedex, France*
[5]*Department of Astronomy, Cornell University, Space Sciences Bldg, Ithaca, New York 14853, USA*
[6]*Department of Planetary Sciences, University of Arizona, 1629 E. University Blvd, Tucson, Arizona 85721, USA*
[7]*Institut für Geologische Wissenschaften, Freie Universität, 12249 Berlin, Germany*
[8]*Department of Space Sciences, Southwest Research Institute, 1050 Walnut Street, Suite 400, Boulder, Colorado 80302, USA*
[9]*Division of Geological and Planetary Sciences, California Institute of Technology, 150-21, Pasadena, California 91125, USA*
[10]*Institute of Planetary Research, German Aerospace Center, Rutherfordstrasse 2, 12489 Berlin, Germany*
[11]*Jet Propulsion Laboratory, California Institute of Technology, 4800 Oak Grove Drive, Pasadena, California 91109, USA*

Titan, the largest moon of Saturn, is the only satellite in the Solar System with a substantial atmosphere. The atmosphere is poorly understood and obscures the surface, leading to intense speculation about Titan's nature. Here we present observations of Titan from the imaging science experiment onboard the Cassini spacecraft that address some of these issues. The images reveal intricate surface albedo features that suggest aeolian, tectonic and fluvial processes; they also show a few circular features that could be impact structures. These observations imply that substantial surface modification has occurred over Titan's history. We have not directly detected liquids on the surface to date. Convective clouds are found to be common near the south pole, and the motion of mid-latitude clouds consistently indicates eastward winds, from which we infer that the troposphere is rotating faster than the surface. A detached haze at an altitude of 500 km is 150–200 km higher than that observed by Voyager, and more tenuous haze layers are also resolved.

In April 2004, as Cassini approached the saturnian system, the Imaging Science Subsystem[1] (ISS) began systematic observations of Titan with a three-month-long sequence, during which the pixel scale improved from ~200 km to 35 km. On 2 July 2004, shortly after entering Saturn orbit, Cassini had a distant (339,000 km) encounter with Titan (referred to as 'T0') during which images of the southern part of the sub-saturnian hemisphere and south-polar region were acquired at pixel scales of 2–3 km. The first close (1,200 km) targeted flyby of Titan ('TA') occurred on 26 October 2004, followed by another close pass with similar geometry ('TB') on 13 December 2004. Both achieved pixel scales of a few hundred metres. These new observations of Titan have major implications for the nature of the surface and atmosphere, and raise important new questions.

Titan's atmosphere consists primarily of nitrogen, with methane being the second-most abundant species (2–6%)[2–4]. Photochemical reactions and escape of the lighter hydrogen produce a rich variety of complex hydrocarbons, which form a haze layer that obscures the surface at visible wavelengths and from which substantial quantities of organics may have precipitated onto the surface[5]. As a result, atmospheric methane has a short photochemical lifetime, suggesting that there is a source or reservoir of methane on or below Titan's surface. At Titan's surface temperature (~94 K) and pressure (1.5 bar), methane and ethane could be liquids, leading to suggestions of rainfall and lakes or seas of light hydrocarbons[6]. Earth-based telescopic observations had revealed bright and dark regions on the surface[7–9] and ephemeral tropospheric clouds[10]. However, we knew very little about either Titan's surface or meteorology.

The new Cassini ISS observations reported here show intricate albedo markings as small as a kilometre on the surface, ~100 times finer than the best Earth-based images. In equatorial regions these markings exhibit east–west and other trends suggestive of aeolian transport and tectonic processes. Concentric or circular albedo patterns that could mark impact structures are rare, suggesting a relatively young surface modified by other geologic and atmospheric processes. Long, curvilinear features, which are primarily dark, but sometimes bright, may mark fluvial channels. However, no enhanced mirror-like (specular) reflections—which would indicate the presence of liquids on the surface—have been detected.

The images have also revealed important information about Titan's atmosphere. In addition to convective clouds in the south-polar (summer) region, we have detected mid-latitude tropospheric clouds. Some cloud features are elongated east–west; these are observed to occur preferentially at certain latitudes and, in the only case where height information is available, at lower altitude than the polar clouds. Tracking of cloud motions consistently yields eastward winds with speeds as high as 34 m s^{-1}, providing the first direct evidence of super-rotation in Titan's troposphere. Upper-atmospheric zonal banding is also apparent, being especially prominent in Titan's north-polar region. A well-defined haze layer is seen at an altitude of 500 km, significantly higher than the 300–350-km altitude layer seen during the Voyager 2 flyby in 1981 (ref. 11), and finer structure is resolved in higher-resolution images of the haze.

On the basis of the chemistry of its atmosphere, Titan is considered to be an important analogue to the early (pre-biotic) Earth[12]. The Cassini ISS observations of Titan's surface suggest another strong similarity between these two bodies: the wide variety

of surface modification processes and their relative importance. Craters on Earth are relatively rare, being quickly modified by tectonism, erosion, burial and volcanism. Furthermore, on Earth all of these processes are continuous, so it is rare to be able to attribute the morphology of a particular region to a single process. Similarly, the diversity of the albedo patterns revealed on Titan's surface suggests a complex interaction between different processes acting concurrently to modify the surface.

Titan's surface

The surface of Titan was barely detected in Voyager visible-wavelength images acquired in 1981 (ref. 13). The Cassini ISS was designed[1] to take advantage of the improved surface visibility at particular infrared wavelengths where the optical depth of the atmospheric haze is lower and where methane gas is not strongly absorbing[14]. Observations acquired during approach were processed to produce a surface map with near-global coverage, except for the unilluminated north (winter) pole (Fig. 1). This map was similar to, but sharper than, the best Earth-based observations at 2.0–2.3 μm (refs 15, 16) where the haze optical depth is low, and it still provides the best-resolution view of the sub-saturnian, equatorial regions. Relatively low-albedo features with scales down to ~100 km, some with strikingly linear boundaries, are seen near the equator, whereas the middle latitudes appear more uniformly bright and the south-polar region is relatively dark. The large bright region centred at 10° S, 100° W has been named 'Xanadu Regio'; this is at present the only officially named feature on Titan.

Images of the southern part of the sub-saturnian hemisphere and south-polar region (2–3 km per pixel) were acquired in the T0 flyby (Fig. 2 and portions of Fig. 1). The low-latitude, large-scale features in these images agree well with the lower-resolution Saturn-approach and Earth-based imaging of Titan's surface, and significantly smaller-scale features are revealed. Several narrow (~10–20 km wide), dark features can be seen to extend for hundreds of kilometres across the surface (Fig. 2b). In some cases these features are relatively straight, suggesting a tectonic influence on the albedo patterns, whereas in others they appear to wind across the surface as might be expected for liquid-carved channels. A broad (~300 km), dark feature runs northward between 330° and 0° W, and there are hints of a concentric pattern of dark, narrow, curvilinear features around the pole. Given the extent to which processes in Titan's atmosphere could affect the surface morphology, the differences between the surface patterns at equatorial and polar latitudes might reflect the cumulative effects of seasonal meteorological variations: for example, channels at high latitudes might be longer, deeper, wider and more extensive as a result of greater precipitation in polar regions (where clouds are currently most abundant).

The close (1,200 km) TA and TB flybys enabled imaging at lower phase angles (≥14°–16°) than in T0 (≥50°), and at much closer ranges. A mosaic of the regional-scale images (Fig. 3) reveals distinct patterns of relatively bright and dark areas. We interpret surface brightness variations, at all scales, as being due to the presence of surface materials with different albedos rather than topographic shading or shadows. Shadows probably cannot be seen from orbit at any phase angle at wavelengths shorter than 1 μm. Even high-phase-angle images (Fig. 2) are likely to reveal only albedo markings for two reasons: (1) an icy satellite of this size is expected to have sufficiently low topographic relief[17] that any shadows or shading would not be detectable at scales of 1–10 km, and (2) the atmospheric scattering must severely reduce the contrast between slope facets facing towards versus away from the direction of the Sun.

The cause of the albedo variations is still not certain, and there may be multiple explanations. It has been hypothesized that the darker regions are accumulations of hydrocarbons (liquid or solid) precipitated from the atmosphere and that the brighter regions are outcrops of water-ice bedrock with variable amounts of contamination[18,19]. (Contaminants weathered from surface exposures of

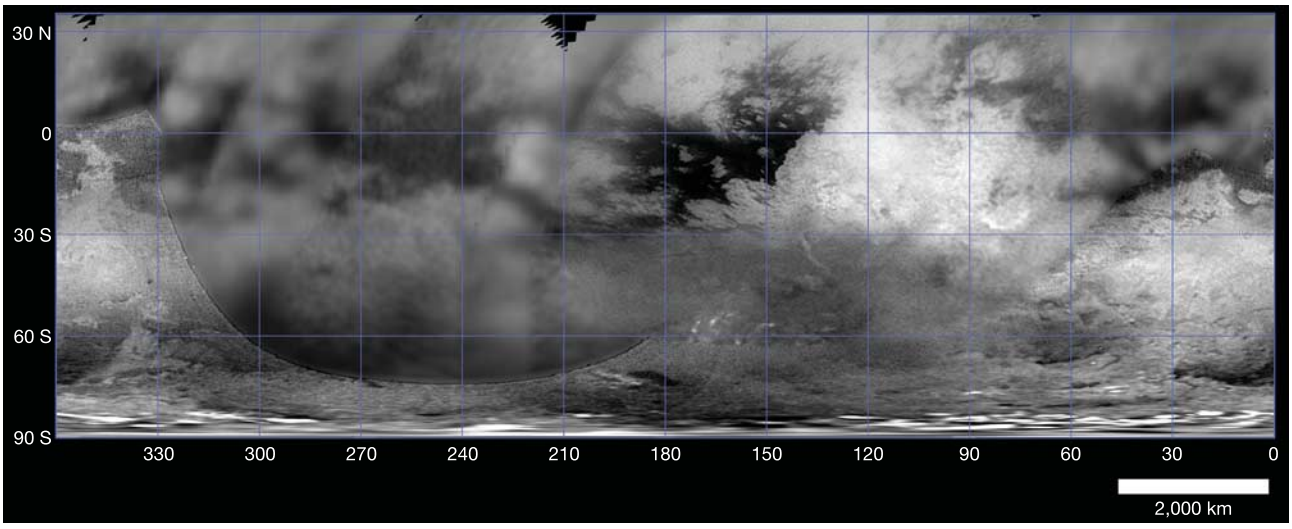

Figure 1 Albedo map of Titan's surface. Near-global, simple-cylindrical map of Titan's surface, assembled from Cassini ISS images taken during approach and the T0, TA and TB flybys. The pixel scales of individual images range from 88 to 2 km, and the corresponding resolutions of surface albedo features range from 176 to ~10 km. The very bright features near the south pole are clouds. High northern latitudes are not illuminated in this season. Unless otherwise noted, images presented here were acquired using the ISS filter that has proved to be most effective at peering through Titan's photochemical haze to its troposphere and surface, a narrow, continuum-band filter (CB3, 938 nm) centred in the best window in methane's absorption spectrum available to the ISS[1]. Because the ISS has two filter wheels, we can also combine CB3 with an infrared polarizing filter, which further reduces the haze contribution at moderate (~90°) phase angles, provided the spacecraft has the proper orientation with respect to Titan and the Sun[1,44]. Images for all surface figures have been processed through the following steps: radiometric calibration; removal of obvious random noise; summation of two or three images to improve the signal-to-noise ratio; division by an image that only detects deep haze, preferably MT1 (619 nm), to normalize brightness variations with illumination and emission angle; improvement of camera-pointing information; re-projection of images to a common map projection; subtraction of 85% of a large-scale smoothed image to approximate atmospheric scattering of photons reflected from the surface; removal of data at very high emission and illumination angles; adjustment of brightness as a function of phase angle and use of polarizing filter; assembly into mosaics; and application of a seam-removal technique that preserves fine detail.

impure ice and transported by fluid flow could contribute to the composition of the darker regions.) This hypothesis and the ISS Titan observations (see below) are consistent with observations made by the Huygens Probe's Descent Imaging Spectral Radiometer (DISR) that indicate that bright areas along the probe's ground-track are relatively high standing and consist of contaminated water-ice, whereas dark areas are lower and have a higher proportion of non-ice material (M. Tomasko, personal communication). Radar measurements from Arecibo Observatory in Puerto Rico revealed a specular component at 75% (12 of 16) of the regions observed (globally distributed in longitude at ~26° S latitude), interpreted as indicative of dark, liquid hydrocarbons[20]. However, there is no correlation between the places where specular signals were detected by Arecibo and the light and dark surface markings observed by the ISS (Fig. 4). There have been no reports to date of specular reflections at visible and near-infrared wavelengths, either by Cassini or Earth-based observers, although the optical depth of the atmosphere at these shorter wavelengths could limit the level at which such enhancement can be detected. That specular detections seem to be confined to radio wavelengths could indicate the presence of surface materials that are smooth at scales of centimetres but rough at scales of micrometres. Temporal variation in the presence of liquids on the surface is another possibility. Analysis of data from Huygens will provide information about the presence of liquid hydrocarbons at the landing site, and further Cassini observations and analyses will help to put these local results into global and temporal context.

Another hypothesis to explain bright and dark regions is that ethane mist might overlie hydrocarbon liquids[14,21], perhaps marking exposures of liquid with bright diffuse features and obscuring specular reflections at optical wavelengths. We might expect such mists to vary in brightness and distribution over time, affected by wind, but comparison of TA and TB images revealed no apparent changes over the seven weeks between these encounters, except for the discrete clouds discussed below.

The albedo variations reveal only a few distinctly circular or concentric patterns that could indicate the presence of large impact structures. A dark annulus (outer edge ~300 ± 20 km) surrounding a bright centre (Fig. 5) could delimit a large impact structure, with the former perhaps filled in part with dark materials in relatively low, confined areas by mass wasting or fluid flow[22]. Impacts by comets should produce a few hundred craters larger than 20 km in diameter per billion years[23]. Furthermore, most of the ejecta from a near-catastrophic breakup of Hyperion was predicted to have struck Titan[24], as would ejecta from other impact events in the saturnian system. We have identified only five prominent

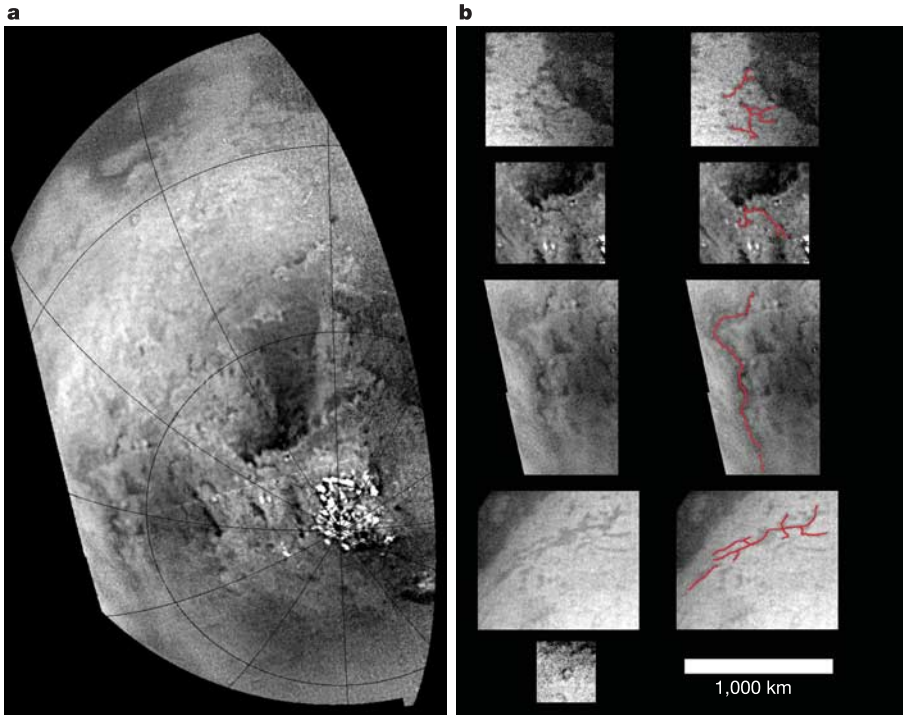

Figure 2 Images of Titan's south polar region. These images were acquired during Cassini's distant T0 encounter on 2 July 2004 and have pixel scales of ~2 km. **a**, A mosaic of Titan's south pole shown in an orthographic map projection. Lines of latitude and longitude are spaced at 30° intervals; the vertical meridian is 330° W. The small bright features near the south pole are clouds; the processing (see Fig. 1 legend) exaggerates their appearance. (The bright narrow line above the polar clouds and extending to the left is a seam in the mosaic.) **b**, Pairs of enlargements from **a** and other T0 images: original images (left) and versions in which some of the narrow, dark, curvilinear and rectilinear surface features, which may be examples of channels and/or tectonic structures, have been traced (right). The longest features (third and fourth pairs from the top) extend for more than 1,000 km across the surface and are as narrow as 10–20 km. At the bottom left, a single frame shows a small dark circular feature, which could be an impact crater. Although the pixel scales of the T0 images were ~2 km, no features smaller than ~10 km are resolved in the images, as expected[1]. Most of the photons detected by the ISS through the CB3 filter have been scattered by the atmospheric haze before ever reaching the surface, and ~60–90% (depending on phase angle and haze properties) of the light that is reflected off the surface from the nadir point (0° emission angle) is scattered by atmospheric haze, spreading the signal over regions up to ~100-km wide. The ~10–40% surface reflection that passes through the atmosphere without scattering (or perhaps via strong forward scattering and relatively little smearing) returns a weak signal, and the modulation transfer function of the Cassini ISS at the Nyquist frequency reduces the contrast over about two pixels by an additional factor of 0.15 (ref. 1). As a result, with reasonable estimates of surface contrast, a single image with an overall signal-to-noise ratio of ~200:1 cannot reveal surface features on scales smaller than about five pixels. The effects of the haze on surface visibility can also be seen by comparison of images showing the same region viewed at different emission angles: at high emission angles (>45°) the surface contrast, and thus effective resolution, is significantly lower than when viewed at low emission angles (for example, Figs 2a and 4).

circular or concentric albedo features larger than 20 km in diameter (Figs 2b, 3, 5, 6a) over the ~30% of Titan imaged at better than 2 km per pixel. In particular, there are three bright circular features 30–50 km in diameter within the dark region west of Xanadu (Fig. 6a), which represents ~5% of the surface area of Titan. Given the lack of topographic information, craters might best be detected by the ISS as albedo features within dark regions where raised crater rims, presumably ice bedrock, would project above the dark infilling material. On the basis of the expected cratering rate[23], if these features are impact structures and we have detected all of the large craters in this region, the age of this part of Titan's surface (that is, the ice bedrock down to a depth of a few kilometres) is only ~130–300 Myr. If large impact structures are this rare on Titan, it suggests that the rates of surface modification processes such as viscous relaxation, tectonic resurfacing, erosion, deposition, and perhaps icy volcanism, have been sufficient to eliminate kilometre-scale relief over timescales of the order of 10^8 years. In contrast, surface ages for Ganymede and Callisto, which are expected to have levels of radiogenic heating comparable to Titan, generally exceed 10^9 years (ref. 23). One possible explanation for a geologically younger surface is that Titan is richer in ammonia, which lowers the melting point of water-ice and makes the resulting liquid neutrally buoyant[25], thereby allowing more extensive endogenic resurfacing at comparable levels of heat flow.

The albedo patterns we do see on Titan's surface are quite varied, and include diffuse bright streaks, narrow dark lineaments (both straight and curved), bright and dark patches with curved or straight edges and often angular boundaries, and dark and bright spots (Figs 3 and 6). It is difficult to identify the processes responsible for many of these patterns, but likely candidates include aeolian and fluvial processes (perhaps sapping), icy volcanism, and tectonics. In many cases a combination of these processes is probably responsible for the features we observe, for example, tectonic structures modified by fluvial activity.

The prominent albedo boundary on the western side of Xanadu varies along its length (Fig. 3). In some places it is quite sharp and exhibits linear and angular shapes (Fig. 6a), whose form and orientation (at this resolution) are consistent with the dark material having embayed the bright terrain, an interpretation in agreement with the DISR findings that the bright regions near the Huygens landing site are higher than the dark regions (M. Tomasko, personal communication).

Streaks are ubiquitous in the equatorial region observed in TA and TB, generally trending west to east (Fig. 3). In addition, many bright patches within the large dark region have sharp western margins and diffuse, elongated eastern margins (Fig. 6b, c), also suggesting eastward flow. Finally, some of the bright patches have streamlined shapes consistent with movement of a fluid from west to east (Figs 3 and 6b). Given the large scale and extent of these features, the atmosphere seems the most likely fluid to be responsible for the patterns. The well-developed eastward pattern is not consistent with a tidal source, because tidal winds should reverse direction twice per Titan day[26]. Instead, the preferred orientation suggests that aeolian features are controlled in some way by the

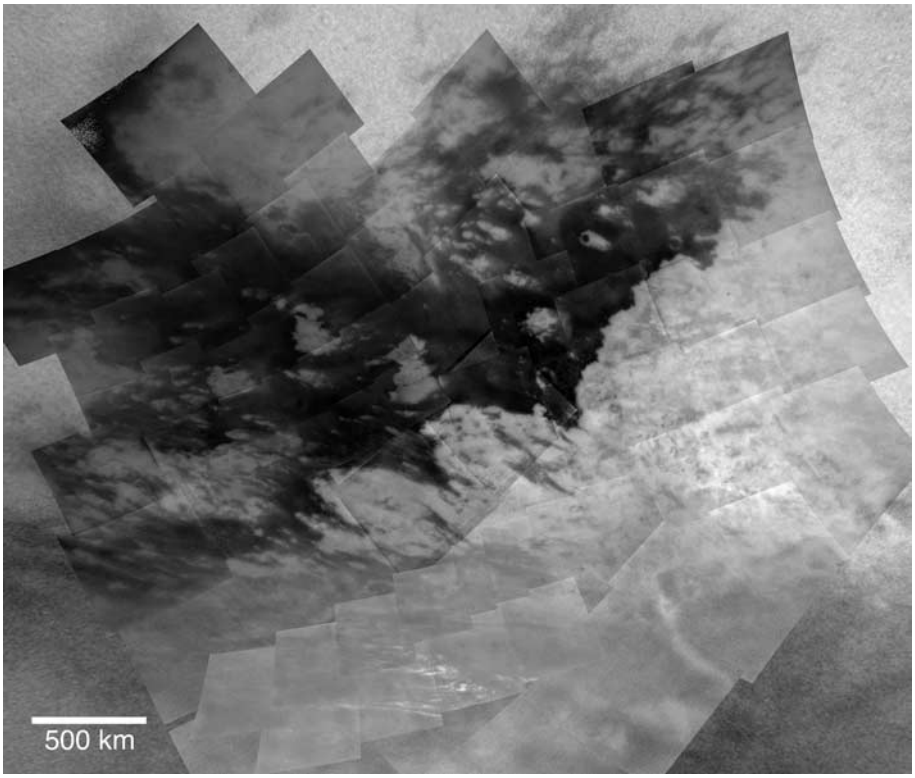

Figure 3 Mosaic of the equatorial region of Titan's anti-saturnian hemisphere. The background is a 3 × 3 mosaic acquired during TA at a scale of ~2 km per pixel (Fig. 4), with closer-range images (0.4–1.2 km per pixel, which means that the approximate scale of features that are resolved is 2–6 km) acquired during TA and TB covering most of the region. This is a simple-cylindrical map projection. Apart from the obvious clouds (described below), which are observed to move and change over timescales of several hours, we are confident that the local brightness variations in CB3 images represent surface features, because: (1) they have well-defined boundaries and have not been observed to change over time; and (2) the larger-scale features agree well with long-term, Earth-based observations and those of the Cassini Visual and Infrared Mapping Spectrometer (VIMS)[45], acquired at longer wavelengths where atmospheric opacity is lower. The top-of-the-atmosphere normalized brightness $\pi I/F$, where I is the intensity corrected to normal illumination and πF is the incident solar flux, varies from 0.26 to 0.39 in the CB3 images without the polarizer filter, but much of this brightness is due to haze. Because the haze is spatially uniform on the scale of the brightness variations, the ratio of the brightest to the darkest surface features is at least $0.39/0.26 = 1.5$. For the brightest surface features $\pi I/F$ is at least 0.13 ($= 0.39 - 0.26$) brighter than the dark material.

observed tropospheric super-rotation (see atmospheric discussion below). Eastward-biased gusts associated with turbulent eddy motions may be the most effective at entraining particles from the surface. Another possibility is wind streaks created as particles settle out of the atmosphere, although accumulation rates are relatively low[27].

Tectonic processes are also likely candidates for shaping Titan's surface: straight and angular lineaments are pervasive at global, regional and local scales (Figs 1, 3 and 6d, respectively). In the bright material on the anti-saturnian hemisphere, prominent lineaments often trend ~N 50° W and ~N 80° E, like conjugate faults (Figs 3 and 6d). One interpretation of these features is large-scale tectonic modification of bright, bedrock material, with accumulations of darker material in low-lying areas enhancing the morphologic patterns (Fig. 6d). Another possibility is that transport of liquids within the ice bedrock results in sapping, which enlarges and darkens tectonic zones of weakness (Fig. 6e), similar to examples seen at closer range by DISR (M. Tomasko, personal communication). However, not all bright features may represent exposures of bedrock. Another hypothesis is that, in places, a thin brittle crust overlies relatively easily deformed dark material (perhaps organic materials precipitated from the atmosphere, although not necessarily in the liquid state[28]), and has been pulled apart or disrupted to expose dark regions (for example, Fig. 6f).

Continued monitoring of Titan may be essential for addressing questions about the causes of the albedo patterns observed on the surface (for example, whether streaks change direction over time, whether bright–dark boundaries change or move over time, whether dark linear features become more or less prominent in different seasons). We see no evidence for changes during the ~50 days between the TA and TB flybys, but changes may yet be seen over longer timescales and would help to constrain the processes responsible.

Titan's clouds and atmospheric dynamics

Methane clouds in Titan's troposphere have been observed in Earth-based images[15]. Before that, they were inferred from variability in near-infrared spectra[10], and had been anticipated on the basis of estimated gaseous methane abundances and lapse rates. Cloud detections in ISS images are limited by the relatively short time intervals available for observations and the infrequent occurrence of clouds in most locations on Titan.

Three different types of clouds have been observed thus far. The most common are fields of small-scale bright clouds near the south pole (Fig. 7a–d), which were present during approach, T0 and TA, but not during TB. Their morphology and evolution is suggestive of cumulus convection. A movie showing the temporal evolution of the polar clouds during the approach to TA can be viewed at http://ciclops.lpl.arizona.edu/view.php?id=537 (global view) or at http://ciclops.lpl.arizona.edu/view.php?id=514 (polar region only). This behaviour is expected given the concentration of solar heating[15] and rising motion at the summer pole[29,30]. Simultaneous images in different filters (Fig. 8) show that the cloud feature is visible in a weak methane band (MT1, 619 nm) and even faintly in a somewhat stronger methane band (MT2, 727 nm). This observation

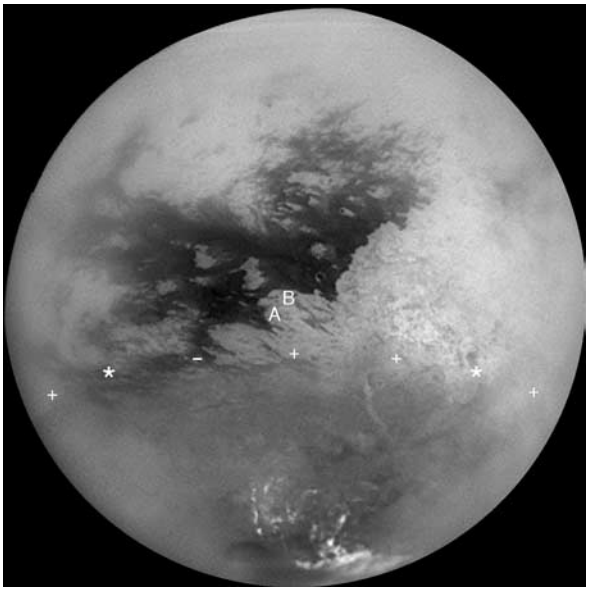

Figure 4 Locations of specular point observations on Titan's anti-saturnian hemisphere. Full-disk 3 × 3 mosaic of images acquired during TA at a pixel scale of ~2 km. The locations of specular points observed by ISS at 938 nm ('A' and 'B' for TA and TB, respectively) and from Arecibo at 13 cm (asterisk for sites of strong specular return and root-mean-square slope less than 1.2; minus sign for no specular component; plus sign for intermediate values of RMS slope) (ref. 20 and D. B. Campbell, unpublished work) are indicated. The TA and TB points are both near bright–dark boundaries, where a specular return could probably be seen from either unit, if there were optically smooth surfaces: for an optical depth of two and a liquid surface roughened by winds of 2 m s^{-1}, the region over which specular reflections would enhance the signal by at least 10% is roughly 200 km across or twice the size of the symbols A and B; for smoother surfaces (lower wind speeds) and/or lower optical depths the area with >10% enhancement can be several hundred kilometres across. Based on the root-mean-square slopes for the two strongest specular returns observed by Arecibo, the echo power comes from regions less than ~100 km across (centred on the sub-Earth point), which is slightly larger than the asterisks. However, owing to the motion of the sub-Earth point during the observation, the extent of the region that is the source of the specular detection represented by the asterisk on the right is known to extend at least 150 km in longitude[20]. For the intermediate values of root-mean-square slope represented by plus signs, the source areas are 250–350 km across, which is 3–4 times the symbol sizes. Signal fluctuations observed at some locations implied structure on scales less than 10 km (ref. 20).

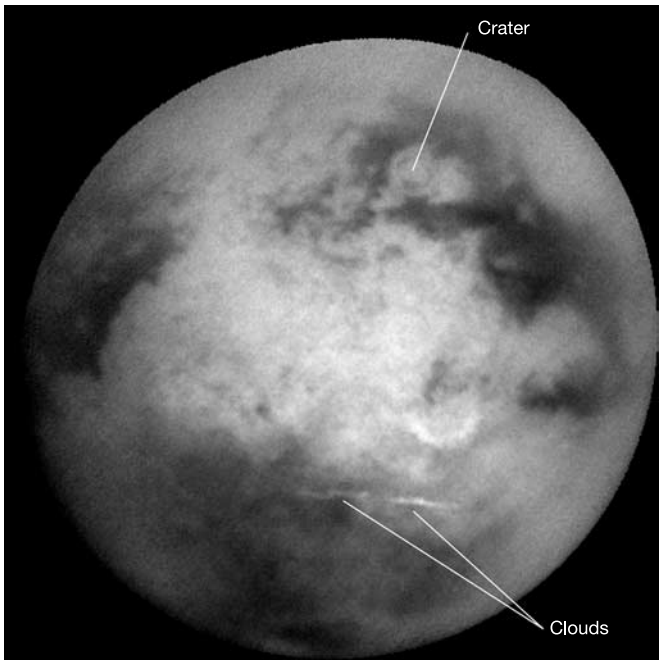

Figure 5 Full-disk image of Titan showing Xanadu Regio. Image acquired on 10 December 2004 during approach to the TB encounter with a pixel scale of 10.4 km. A concentric albedo pattern, perhaps an impact structure, can be seen within the dark region northeast of Xanadu Regio (bright region in centre of disk). The outer edge of the dark annulus has a diameter of 300 ± 20 km. Flow-like patterns southwest of this concentric feature could indicate sites of icy volcanism. Two bright, linear clouds are present just to the south of Xanadu.

suggests that the polar cloud tops are at high tropospheric altitude. Earth-based inferences suggest cloud tops as high as ~25 km (ref. 15).

A second, rarer cloud class is discrete mid-latitude clouds[31,32] (Fig. 7e–g). These clouds tend to be small and faint and persist for only a few hours. We have thus far tracked cloud motions in 12 discrete mid-latitude and polar clouds using a digital tracking technique[33]. Prograde (eastward) winds are measured for ten of the 12 clouds, the other two being motionless over the few-hour time interval (Fig. 9). The fastest wind speed recorded to date is $34 \pm 13\ \mathrm{m\,s^{-1}}$ at 38° S latitude.

These wind vectors are the first direct evidence for Titan tropospheric super-rotation (atmosphere rotating faster than the surface), which had been inferred from Voyager temperature gradients[34] and predicted by models[29,30,35,36]. Prograde winds can be produced by displacing rings of air from the equator to higher latitudes and conserving angular momentum, for example, in the near-tropopause branch of a Hadley cell. The cloud motions we measure are probably from lower levels where winds are slower, but two of our wind vectors are faster than an angular-momentum-conserving profile (Fig. 9, dashed curve). A Hadley cell cannot produce such wind speeds if the rings of air are motionless at the equator, suggesting that eddy momentum transport is important in maintaining super-rotation on Titan[35].

Uniform angular momentum in the troposphere would require an unrealistically large meridional temperature gradient[37]. Uniform atmospheric angular velocity relative to the surface (wind varying as cosine latitude) is more consistent with the small meridional surface temperature contrast inferred by Voyager[34] and more like the low-level super-rotation observed on Venus[37] and simulated by one Titan model[30]. This would imply equatorial super-rotation speeds of tens of metres per second in the middle troposphere. Possible aeolian surface features implying eastward flow at low latitudes (Figs 3 and 6b) are also consistent with equatorial super-rotation.

The third class of cloud features consists of large-scale nearly zonal streaks (Figs 3 and 5). The 11 streak clouds observed to date

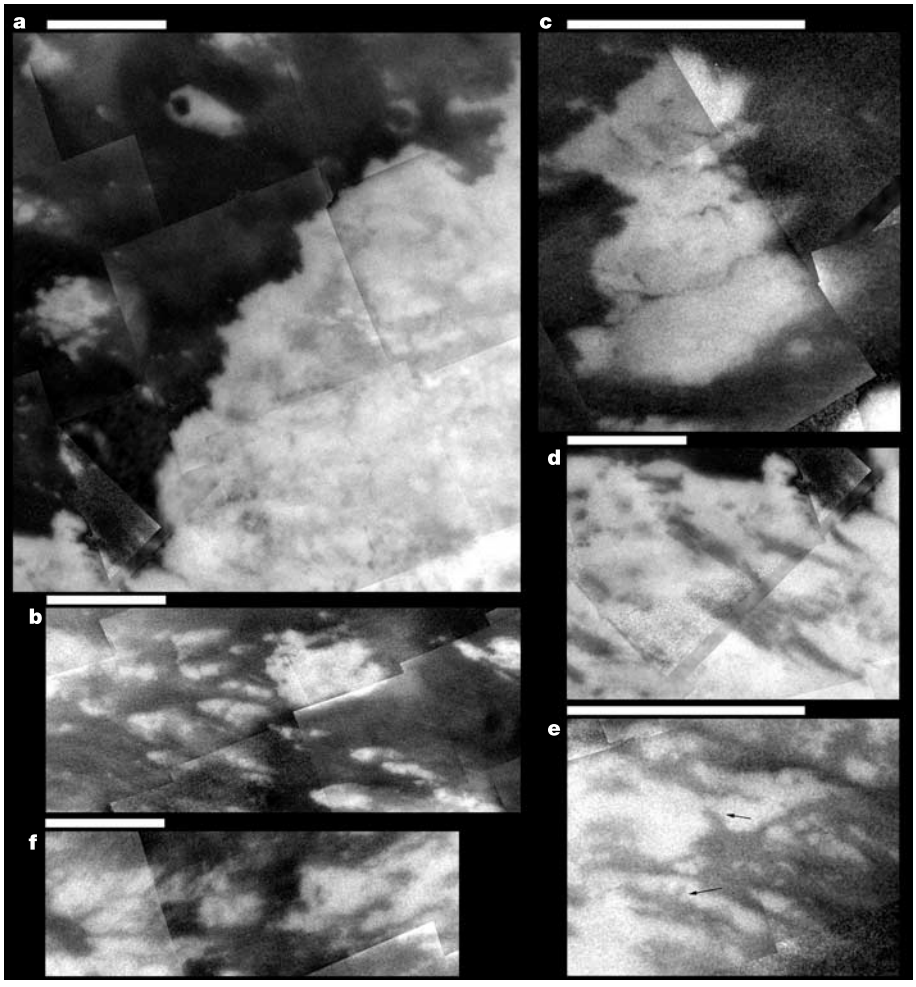

Figure 6 High-resolution views of Titan's surface. These enlarged views from the mosaic in Fig. 3 all have north to the top of the frame. White bars above each image are 200 km long. (Sharp lines are seams between individual images that have not been completely removed.) **a**, Prominent bright–dark boundary near the western edge of Xanadu exhibiting a sharp, angular contact between the two albedo units. Eastward-oriented, acute angles are common. The two bright, discontinuous circles, which could be impact structures, within the dark material near the top of the image are approximately 30 km in diameter and another near the lower left of the image is ~50 km in diameter. **b**, Streamlined bright features consistent with fluid motion from west to east. The Huygens landing site is in the upper left corner of this image. The region is in the centre left of Fig. 3. **c**, Bright feature (near the centre of Fig. 3) surrounded by dark material, illustrating the contrast between the sharp western boundary and more diffuse eastern boundary. Several narrow (~2 km), dark lanes cross the bright area and the western bright–dark boundary exhibits acute angles as in **a**. **d**, Dark, linear lanes in this region west of Xanadu suggest a tectonic influence on the surface morphology, perhaps enhanced by other processes. **e**, Albedo patterns in this region southeast of the Huygens landing site (note arrows) exhibit shapes suggestive of erosion by sapping. **f**, A region near the upper right of Fig. 3 showing bright patches that could be reconstructed as though a bright crust has been extended east–west over a dark substrate.

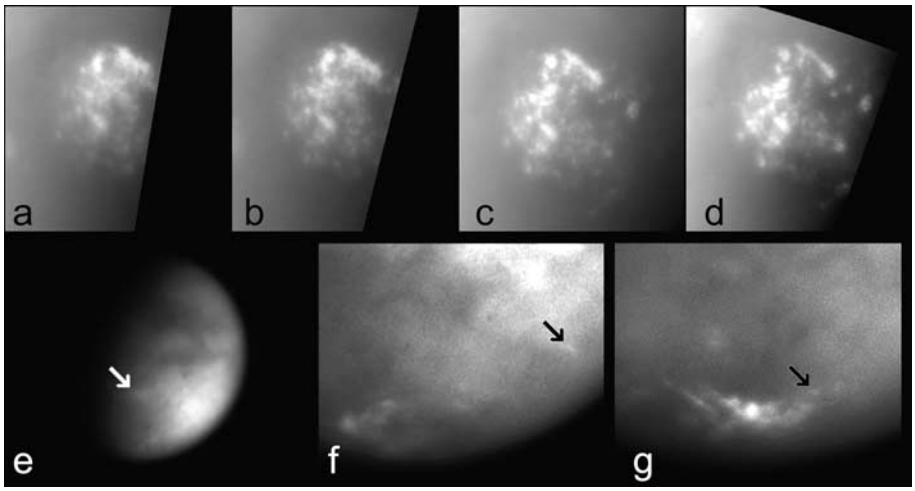

Figure 7 Tropospheric cloud features on Titan. **a**–**d**, A sequence of four methane continuum (IRP0-IR3, 928 nm) images showing the temporal evolution over the period 05:05–09:38 of the Titan south polar cloud field on 2 July 2004. **e**–**g**, Three examples of discrete mid-latitude clouds (arrows) for which motions have been tracked in CB3 images. **e**, 38° S, 81° W (29 May 2004); this image was also viewed through an infrared polarizing filter. **f**, 43° S, 67° W (23 October 2004); **g**, 65° S, 110° W (25 October 2004). The clouds in **f** and **g** can also be seen briefly in the TA approach movies (see text for URLs).

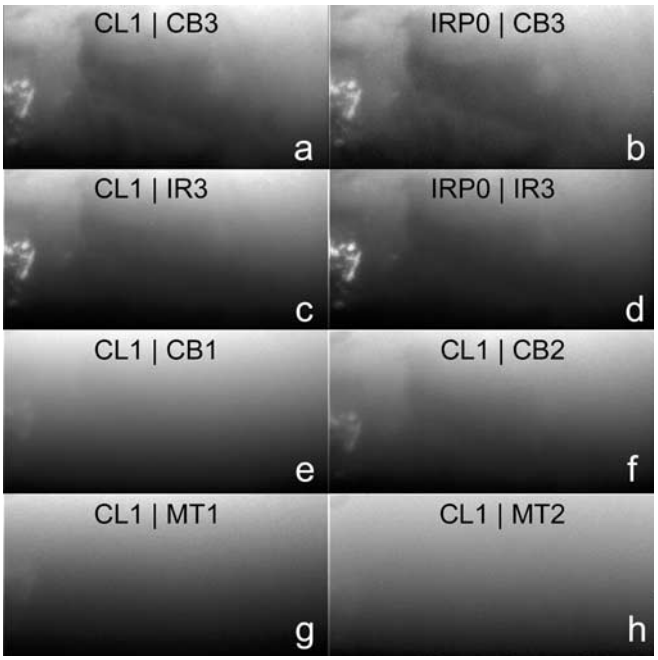

Figure 8 South polar clouds seen at different wavelengths. Near-simultaneous images of Titan's south polar regions acquired on 2 July 2004 in eight filter combinations, as indicated by the legend at the top of each image. The high-contrast cloud feature on the left of each image is located at the south pole. For each image, a spectral bandpass filter was combined with either a clear filter (CL1) or an infrared polarizing filter (IRP0), which helps reduce obscuration by the overlying stratospheric haze. Filters are as follows: Narrowband methane continuum images (CB3, 938 nm) without (**a**) and with (**b**) the polarizing filter. Broadband infrared (IR3, 928 nm) images, without (**c**) and with (**d**) the polarizing filter. **e**, **f**, Narrowband methane continuum images CB1 (635 and 603 nm; **e**) and CB2 (750 nm; **f**). **g**, **h**, Methane band images in weak (MT1, 619 nm; **g**) and moderate strength (MT2, 727 nm; **h**) bands. Both clouds and apparent surface features are visible in CB3 and IR3 and to a lesser extent in CB2 and CB1, for which obscuration by stratospheric haze is stronger. In MT1, all features except the polar clouds have disappeared. Gas absorption alone is sufficient to ensure that fewer than 1% of MT1 photons reach the surface, and haze scattering reduces this further. The cloud is barely visible in MT2, which has essentially no contribution from the surface.

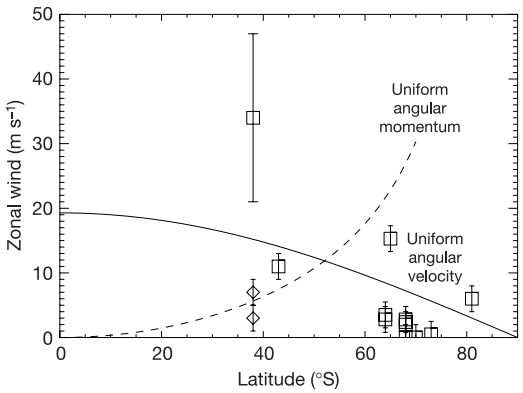

Figure 9 Cloud-tracked wind speeds versus latitude on Titan. The wind vectors probably refer to middle- and lower-troposphere altitudes. Squares indicate discrete clouds, and diamonds indicate streak clouds. The vertical lines are root-sum-square error bars for each wind speed. Latitude uncertainty is slightly smaller than the symbol widths. The scatter is due to real temporal variability, clouds at different altitudes with different mean winds, and tracking uncertainty. Wind speed uncertainty is the result of pixel resolution, navigation errors and cloud evolution. For clouds observed during the flybys, the pixel-resolution contribution is negligible (0.1 m s^{-1}). Navigation error is estimated by measuring displacements of nearby surface features; the worst-case error is 0.6 m s^{-1}. The largest error is due to cloud shape changes. We estimate a total wind speed uncertainty of 2 m s^{-1} based on changes in estimates for one feature at different times and differences between two tracking estimates. For the mid-latitude cloud feature seen on approach, pixel resolution is the dominant error source (9 m s^{-1}). Navigation error is much smaller, because digital tracking measures zero displacement of surface features in the same images. Assuming cloud evolution error to be less than one pixel, based on the correlation map, the total uncertainty is 13 m s^{-1}. The solid curve is a uniform angular velocity profile for the area-weighted mean angular velocity of all moving discrete features. It implies an equatorial super-rotation speed of 19 ± 15 m s^{-1}, with most of the uncertainty probably due to real variation of wind speed with altitude. The dashed curve is a uniform angular momentum profile for a parcel with zero wind velocity at the equator. An angular-momentum-conserving profile consistent with our fastest wind vector implies a lower limit for the equatorial super-rotation of 22 ± 10 m s^{-1}.

occur at preferred latitudes (six occurrences at 36–39° S, three at 67–72° S) and longitudes (all but two between 50–200° W), but examples exist at 14° S and 33° S as well. Cloud streaks are also seen in ground-based images at similar times[32]. The streak morphology and distribution invites three interpretations: (1) shearing and stretching by rapid upper-level super-rotating winds; (2) association with surface methane sources, for example, venting of methane gas from a subsurface reservoir through cracks in the surface; and (3) orographic waves generated by meridional flow over zonally oriented topography.

Each interpretation is problematic. Methane band images were available for one streak during TB, but it was not detected in MT2, indicating that it was at lower altitude than the polar clouds and thus less subject to shearing by strong winds. Two mid-latitude streaks were tracked at speeds of less than 10 m s^{-1} (Fig. 9), also implying tops at lower levels than other clouds and making it difficult to explain their large zonal extent unless these speeds are atypical. Some streaks curve slightly poleward from west to east, consistent with the expected sense of the summer lower troposphere meridional flow. Thus, generation from a surface source seems more likely, especially since streaks occur in preferred regions. If so, the images do not yet identify the source. Medium-resolution images of a streak location during TB taken at a time when the streak was absent (TA) revealed no distinctive surface features, but cracks or topography finer than the ~1-km effective ISS surface resolution cannot be ruled out.

Titan's stratospheric haze

Our early observations of Titan were made almost exclusively with filters at long or short wavelengths to optimize our chances of seeing the surface and tropospheric clouds or contrasts in the stratosphere, which would provide a basis for tracking motions. Images of the southern hemisphere with the UV3 filter (338 nm) showed no contrast, unlike images taken in 2003 using a similar filter on the Hubble Space Telescope[38] (HST) that do show a darker south polar hood. However, the HST images show that polar hood contrast decreased recently. The absence of contrast in Cassini images from April–July 2004 is consistent with that trend.

In UV3 images a faint thin haze layer encircles the denser stratospheric haze (Fig. 10a). Radial profiles of normalized intensity for this image (Fig. 11) suggest that the thin haze is similar to a 'detached' haze layer seen in Voyager images[11], but the altitude of the

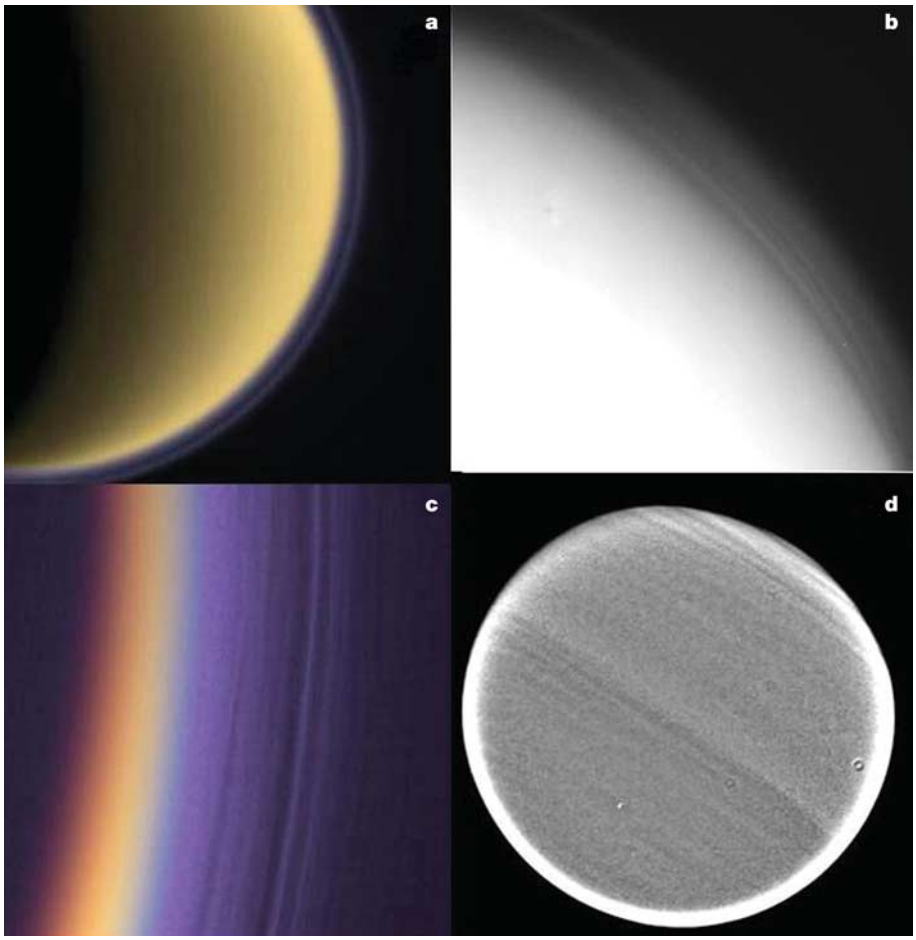

Figure 10 Images of Titan's stratospheric haze layers. **a**, Titan's southern polar region seen in the UV3 (338 nm) filter. The image is false-coloured to approximate what the human eye might see were our vision to extend into the ultraviolet: The globe of Titan retains the pale orange hue in the visible, and both the main atmospheric haze and thin detached layer are given their natural purple colour. The haze layers are brightened for visibility. The image was taken on 3 July 2004 at a Sun–Titan–spacecraft angle (or 'phase angle') of 114°. The pixel scale is 4.7 km. **b**, Titan's spin axis is tipped ~45 degrees to the vertical in this UV3 image of the northern polar hood. Multiple layers are seen between about 200 and 500 km altitude. **c**, A composite of a Cassini UV3 image of Titan's nightside limb, and BL1 (451 nm), GRN (568 nm), and RED (650 nm) filters taken within 4 min of each other on 13 December 2004. They have been combined to look like true colour and stretched in brightness. The pixel scale is 0.7 km and the phase angle is 162°. The limb shown is at ~10° S latitude. Although this is a nightside view, with only a thin crescent receiving direct sunlight, the haze layers are bright from light scattered through the atmosphere. About 12 distinct haze layers can be seen extending several hundred kilometres above the surface. **d**, A methane filter (MT3, 890 nm) image shows faint horizontal banding at several latitudes, most prominently at northern high latitudes. The image was high-pass-filtered to enhance very weak contrasts at high spatial frequency. Consequently the limb appears very bright and there are circular features from dust on the optics—both artefacts amplified by the process.

haze observed by Cassini (near 500 km) is significantly higher than the detached haze seen by Voyager (300–350 km). One model suggests that the detached haze is produced by dynamics and haze sedimentation acting directly beneath the production altitude (which is specified to give the Voyager result)[30]. The upward shift in haze altitude we observe thus suggests the possibility of seasonality in haze production or circulation strength, not captured by the existing models[39].

Images also reveal a multi-layer structure in the north polar hood region (Fig. 10b). The circle defined by the detached haze forms the top boundary of a set of arcs seen most readily in UV3 images. These arcs are not all mutually aligned, and two of them appear to merge. It is difficult to determine whether these are vertically distinct, individual haze layers or a manifestation of fewer layers with an altitude undulation that is accentuated in the near-terminator geometry of the north polar hood. Layering at lower latitudes is also seen in transmitted light looking back at high phase angle (Fig. 10c). These features might be produced by gravity waves, which have been detected previously at lower altitudes[40,41]. Advection by the oscillating vertical component of wave motion in a haze of vertically varying concentration might make such waves visible. The vertical wavelength appears to decrease with altitude (Fig. 12). This behaviour would be expected if the atmosphere became more thermodynamically stable with height, but these waves seem to be located in Titan's upper stratosphere/lower mesosphere where stability decreases with height. A more likely explanation for the decreasing wavelength, if real, is that the phase speed of the waves relative to the background zonal winds decreases upward as the super-rotation strengthens.

Higher-resolution images at high phase angle show many individual layers at low and middle latitudes, especially in the UV3 filter (Fig. 10c) but also in longer-wavelength filters. This and other images at high spatial resolution and high phase angle show undulations along the limb (apparent edge of the disk). These undulations are perhaps also a manifestation of a perturbing gravity wave. Structure is seen in the stratospheric haze against the disk with the MT3 (889N) filter, which samples the strong 890-nm methane absorption band. Weak contrasts with a strong zonal (axisymmetric) pattern are seen (Fig. 10d) and are most prominent at high northern latitudes. The contrasts are confined to the stratosphere at pressures <150 mbar. Their strong zonal nature suggests a stratosphere dominated by zonal flow, as models predict[29,30]. Eddies and meridional motion, if they exist at this level, are too weak to be detected.

Two global inversion layers above an altitude of 400 km have been inferred from analysis of stellar occultations[42]. These may well be related to the some of the layering we see. The inversions are at pressures of a few microbars where the sedimentation velocities of aerosols are high, so the new observations will be a challenge to aerosol microphysical models.

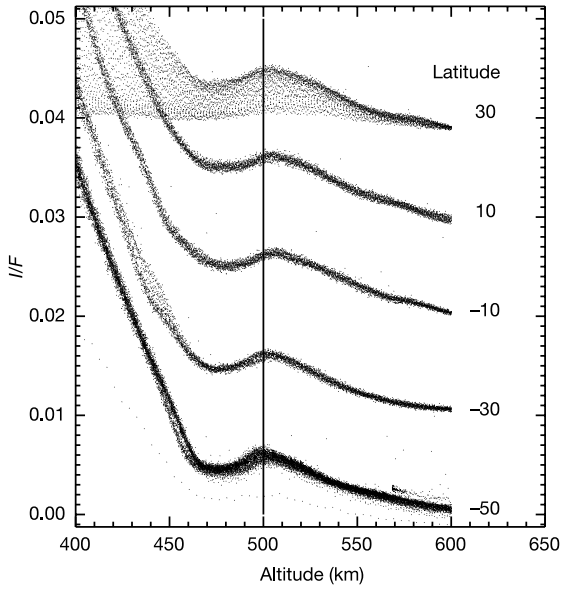

Figure 11 Intensity profiles of Titan's detached haze layer at varying latitudes. Reflected UV3 intensity (I/F) for five latitude bands versus altitude above Titan's surface. Latitude is defined as the latitude of the surface directly below the tangent point of the ray path that samples the stratosphere. Plots for latitudes north of $-50°$ are offset by increments of 0.01 for clarity. Each set of points is selected from a bin 10° wide centred on the latitude shown. The points in the 30° bin include some near the terminator with low I/F values. Otherwise relative uncertainty can be gauged by the spread in the data for each profile, although there is a contribution from latitude variation and navigation uncertainty. Altitudes are sensitive to the position of Titan's centre in the image, which is uncertain to ± 3 pixels (about ± 15 km). There is also an I/F uncertainty of about ± 0.003 because the procedure for background subtraction was inexact. The images should also be deconvolved with the camera point spread function, which is expected to change the profiles slightly (the trough near 470 km will deepen and intensities will decrease faster above 500 km). However, these effects will not significantly change the altitude of the local I/F peak that defines the detached haze. The altitude of the detached haze was also measured from an image taken in late October when the phase angle was low and the detached layer was visible over most of the 360° of azimuth around the sub-spacecraft point. It is not visible as a detached layer in the polar hood region, but the circle fitted to the haze outside the polar hood also defines the boundary of the polar haze. This circle corresponds to an altitude of 507 km above Titan's surface.

Discussion

Cassini's early imaging observations of Titan have begun to yield insights into the nature of its surface and atmosphere. Titan is a complex world, which appears to be influenced by tectonic, fluvial and atmospheric processes, in many ways similar to Earth, although the rates of such activity may be much slower on Titan.

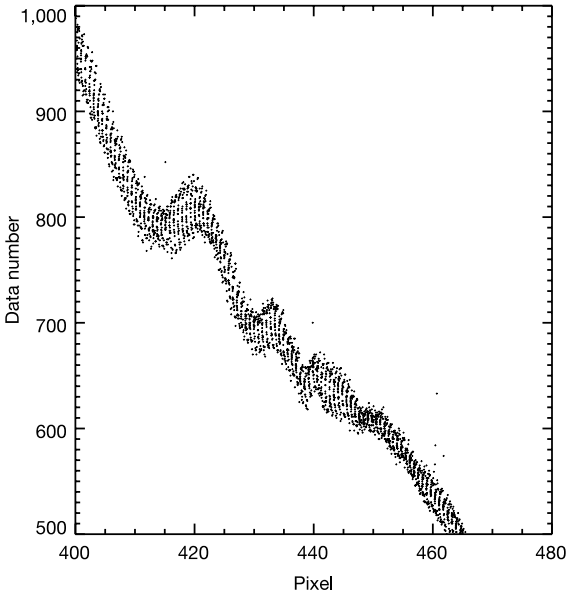

Figure 12 Multiple haze layers in Titan's north polar hood. Relative intensity (data number) in a radial direction from an altitude of approximately 200 to 500 km above the north pole of Titan. The layers seen in the image (Fig. 10b) appear here as local maxima in a downward-trending profile. The very weak local maxima and minima at sample numbers higher than 30 are visible as layers in the image. Altitude increases to the right. The relative uncertainty in the data number values can be judged from the vertical distribution of points. The data are taken from an unprocessed raw image.

The albedo patterns revealed on Titan's surface suggest that tectonics, viscous relaxation, aeolian, and perhaps fluvial processes have played significant roles in surface modification, although the ISS has yet to find direct evidence for surface liquids. Titan's current atmosphere inhibits the formation of impact craters of diameters less than ~20 km (ref. 43), so a lack of craters of these sizes would require either that the present atmosphere has persisted over a substantial part of Titan's history, or that the rate of surface modification has (at least recently) been rapid enough to remove or obscure smaller craters. However, large impact structures also appear to be rare, especially in comparison to the surfaces of other saturnian satellites, so other surface processes must remove kilometre-scale relief over timescales of 10^8 years. Furthermore, the widespread presence of linear features in equatorial regions implies that the long-term rates of tectonism must be comparable to, or greater than, those of erosion and deposition. Although spatial coverage by ISS is still somewhat limited, the overall style of the observed albedo patterns seems to vary with latitude, which may reflect differences in the cumulative effects of atmospheric processes that influence the surface. The analysis of Huygens data will provide important detailed information to aid our interpretations, and with continued Cassini observations we will build up a global view of Titan from which it will be possible to assess the various surface-modification processes at work and their relative importance. We will also be able to investigate the interactions between the surface and the atmosphere and look for changes as spring approaches in Titan's northern hemisphere.

Cassini images have also documented super-rotating winds in Titan's troposphere at mid-latitudes, verifying the predictions of general circulation models[29,30,35,36]. Clouds and wind information at low latitudes is lacking at present, presumably because upwelling is concentrated at high latitudes in summer. If so, clouds might begin to occur at lower latitudes as Titan approaches the vernal equinox[32], allowing equatorial super-rotation to be measured directly and compared with that observed by Huygens, and the possible role of precipitation in modifying the surface to be evaluated. Determining the vertical profile of the winds we measure will require quantifying cloud top altitudes, using radiative models constrained by methane abundance and stratospheric haze properties derived from Huygens data.

The altitude of Titan's detached stratospheric haze needs to be monitored as Titan approaches the equinox to determine whether the Voyager–Cassini difference is seasonal. The current results already provide a challenge to photochemical models to explain the factors that control the peak haze-production altitude and the processes that remove haze particles from the stratosphere. Such models are needed to estimate the downward flux of organics that may supply dark material to Titan's surface. □

Received 11 January; accepted 7 February 2005; doi:10.1038/nature03436.

1. Porco, C. C. *et al.* Cassini imaging science: Instrument characteristics and anticipated scientific investigations at Saturn. *Space Sci. Rev.* **115,** 363–497 (2004).
2. McKay, C. P. *et al.* Temperature lapse rate and methane in Titan's troposphere. *Icarus* **129,** 498–505 (1997).
3. Samuelson, R. E., Nath, N. R. & Borysow, A. Gaseous abundances and methane supersaturation in Titan's troposphere. *Planet. Space Sci.* **45,** 959–980 (1997).
4. Lunine, J. I. & Soderblom, L. A. Cassini-Huygens investigations of satellite surfaces and interiors. *Space Sci. Rev.* **104,** 191–208 (2002).
5. Khare, B. N., Sagan, C., Bandurski, E. L. & Nagy, B. Ultraviolet-photoproduced organic solids synthesized under simulated jovian conditions: Molecular analysis. *Science* **199,** 1199–1201 (1978).
6. Lunine, J. I., Stevenson, D. J. & Yung, Y. L. Ethane ocean on Titan. *Science* **222,** 1229–1230 (1983).
7. Smith, P. H., Lemmon, M. T. & Lorenz, R. D. Titan's surface, revealed by HST imaging. *Icarus* **119,** 336–349 (1996).
8. Coustenis, A. *et al.* Images of Titan at 1.3 and 1.6 μm with adaptive optics at the CFHT. *Icarus* **154,** 501–515 (2001).
9. Gibbard, S. G. *et al.* Speckle imaging of Titan at 2 microns: surface albedo, haze optical depth, and tropospheric clouds. *Icarus* **169,** 429–439 (2004).
10. Griffith, C. A. *et al.* Transient clouds in Titan's lower atmosphere. *Nature* **395,** 575–578 (1998).
11. Rages, K. & Pollack, J. B. Vertical distribution of scattering hazes in Titan's upper atmosphere. *Icarus* **55,** 50–62 (1983).
12. Raulin, F. & Owen, T. Organic chemistry and exobiology on Titan. *Space Sci. Rev.* **104,** 377–394 (2002).
13. Richardson, J., Lorenz, R. D. & McEwen, A. Titan's surface and rotation—New insights from Voyager images. *Icarus* **170,** 113–124 (2004).
14. Griffith, C. A., Owen, T. & Wagener, R. Titan's surface and troposphere, investigated with ground-based, near-infrared observations. *Icarus* **93,** 362–378 (1991).
15. Brown, M. E., Bouchez, A. H. & Griffith, C. A. Direct detection of tropospheric clouds near Titan's south pole. *Nature* **420,** 795–797 (2002).
16. Bouchez, A. *et al.* Keck Observatory Titan monitoring project. ⟨http://www2.keck.hawaii.edu/science/titan/⟩ (2005).
17. Perron, J. T. & de Pater, I. Dynamics of an ice continent on Titan. *Geophys. Res. Lett.* **31,** doi:10.1029/2004GL019802 (2004).
18. Lorenz, R. D. & Lunine, J. I. Titan's surface before Cassini. *Planet. Space Sci.* (in the press) (2005).
19. Griffith, C. A. *et al.* Evidence for exposure of water ice on Titan's surface. *Science* **300,** 628–630 (2003).
20. Campbell, D. B. *et al.* Radar evidence for liquid surfaces on Titan. *Science* **302,** 431–434 (2003).
21. Lunine, J. I. Does Titan have an ocean? A review of current understanding of Titan's surface. *Rev. Geophys.* **31,** 133–150 (1993).
22. Lorenz, R. D. Crater lakes on Titan: rings, horseshoes, and bullseyes. *Planet. Space Sci.* **42,** 1–4 (1994).
23. Zahnle, K., Schenk, P., Levison, H. & Dones, L. Cratering rates in the outer Solar System. *Icarus* **163,** 263–289 (2003).
24. Dobrovolskis, A. R. & Lissauer, J. J. Fate of ejecta from Hyperion. *Icarus* **169,** 462–473 (2004).
25. Croft, S. K., Lunine, J. L. & Kargel, J. Equation of state of ammonia-water liquid—Derivation and planetological applications. *Icarus* **73,** 279–293 (1988).
26. Tokano, T. & Neubauer, F. M. Tidal winds on Titan caused by Saturn. *Icarus* **158,** 499–515 (2002).
27. Strobel, D. F. Chemistry and evolution of Titan's atmosphere. *Planet. Space Sci.* **30,** 839–848 (1982).
28. Dimitrov, V. & Bar-Nun, A. Hardening of Titan's aerosols by their charging. *Icarus* **166,** 440–443 (2003).
29. Hourdin, F. *et al.* Numerical simulation of the general circulation of the atmosphere of Titan. *Icarus* **117,** 358–374 (1995).
30. Rannou, P. *et al.* A coupled dynamics-microphysics model of Titan's atmosphere. *Icarus* **170,** 443–462 (2004).
31. Lemmon, M. T. *et al.* HST observations of Titan, 1994–1997: New surface albedo maps and detection of large-scale, sub-tropical cloud activity. *Icarus* (submitted).
32. Roe, H. G. *et al.* Discovery of temperate latitude clouds on Titan. *Astrophys. J.* **618,** L49–L52 (2005).
33. Rossow, W. B., Del Genio, A. D. & Eichler, T. P. Cloud-tracked winds from Pioneer Venus OCPP images. *J. Atmos. Sci.* **47,** 2053–2084 (1990).
34. Flasar, F. M., Samuelson, R. E. & Conrath, B. J. Titan's atmosphere: Temperature and dynamics. *Nature* **292,** 693–698 (1981).
35. Del Genio, A. D., Zhou, W. & Eichler, T. P. Equatorial superrotation in a slowly rotating GCM: Implications for Titan and Venus. *Icarus* **101,** 1–17 (1993).
36. Del Genio, A. D. & Zhou, W. Simulations of superrotation on slowly rotating planets: Sensitivity to rotation and initial condition. *Icarus* **120,** 332–343 (1996).
37. Allison, M., Del Genio, A. D. & Zhou, W. Zero potential vorticity envelopes for the zonal-mean velocity of the Venus/Titan atmospheres. *J. Atmos. Sci.* **51,** 694–702 (1994).
38. Lemmon, M., Smith, P. & Lorenz, R. The evolution of Titan's polar hood near summer solstice. *35th COSPAR Scientific Assembly (Paris, 18–25 July 2004)* abstr. COSPAR04-A-04048 (2004).
39. Hutzell, W. T. *et al.* Simulations of Titan's brightness by a two-dimensional haze model. *Icarus* **119,** 112–129 (1995).
40. Hinson, D. P. & Tyler, G. L. Internal gravity waves in Titan's atmosphere observed by Voyager radio occultation. *Icarus* **54,** 337–352 (1983).
41. Friedson, A. J. Gravity waves in Titan's atmosphere. *Icarus* **109,** 40–57 (1994).
42. Sicardy, B. *et al.* The structure of Titan's stratosphere from the 28 Sgr occultation. *Icarus* **142,** 357–390 (1999).
43. Korycansky, D. G. & Zahnle, K. J. Modeling crater populations on Venus and Titan. *Planet. Space Sci.* (in the press).
44. West, R. A. & Smith, P. H. Evidence for aggregate particles in the atmospheres of Titan and Jupiter. *Icarus* **90,** 330–333 (1991).
45. Sotin, C. *et al.* Cassini VIMS observations during the October 2004 flyby of Titan: Clues to the dynamics of Titan's surface. *Nature* (submitted).

Acknowledgements We acknowledge the many members of the imaging team who have assisted in the design of imaging sequences and camera commands and in other vital operational and image processing tasks, in particular N. Martin, E. Birath, J. Riley, B. Knowles, C. Clark, M. Belanger and D. Wilson. This work has been funded by NASA/JPL, the UK Particle Physics and Astronomy Research Council, the German Aerospace Center (DLR), and Université Paris VII Denis Diderot, CEA, AIM, France.

Competing interests statement The authors declare that they have no competing financial interests.

Correspondence and requests for materials should be addressed to C.C.P. (carolyn@ciclops.org).